Boundary Condition Scaling for Short Characteristics in SPECT3D

In the Long Characteristics (LC) model of radiation transfer in plasmas, each plasma cell is given a grid of angles, each of which produces a ray from the plasma edge to the cell centroid. Radiation transport is calculated along the full length of each ray and averaged for the cell-centered intensity. Short Characteristics (SC) is an approximate method where explicit transport is calculated only out to N cell intersections for each ray. At the N-intersection ray termination, the boundary condition is defined by the intensity in the cell which is at that termination, at the closest angle (or average of closest angles). Thus, rays which terminate at the plasma edge (where radiation is given) must be calculated first, so that they may be used as boundary conditions when needed. See the Appendix "Short-N Characteristics method" for more details.

While SC can save immensely in computation time, the major sacrifice in accuracy is due to a different ultimate path through the plasma. In general, the SC route through the plasma adds up to a longer total path than the straight line in LC. An example is shown in Figure 1 for a 2DRZ plasma. The gridlines are plasma cell boundaries in the RZ plane. For the cell bordered in magenta, a particular angle is shown in blue for LC path, and red for the sequence of SC path segments which lead to the boundary condition for the N-intersection ray for this cell. It is clear by eye that path is longer in the SC case.

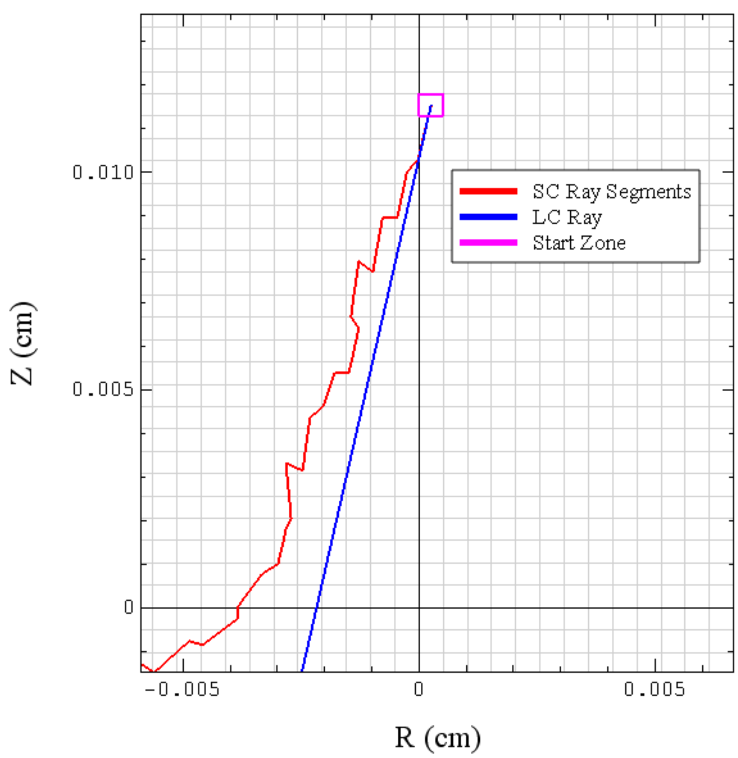

Figure 1. Example of an effective SC path (red) vs. a LC path (blue).

While SC paths in 2DRZ geometry tend to be complex due to the added challenge of closest angle finding, Figure 2 demonstrates that this effect still occurs in the simpler case of 2DXY geometry.

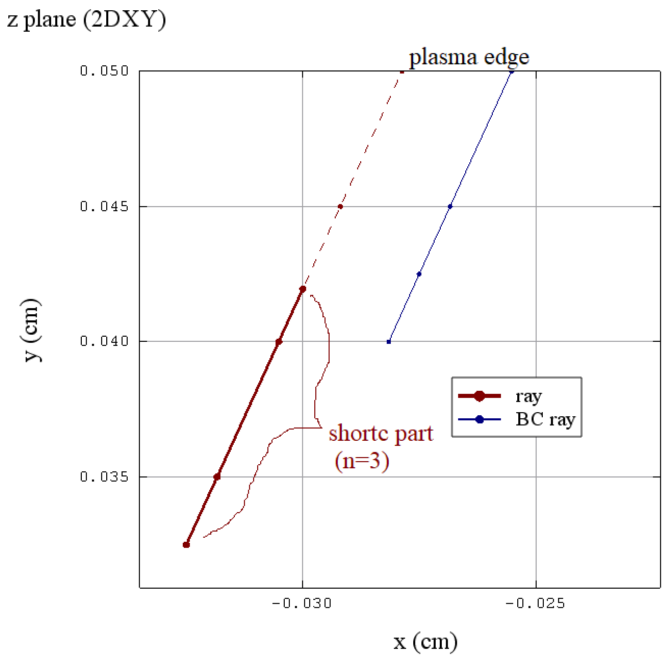

Figure 2. Example of additional total path length introduced by SC steps in 2DXY geometry.

When optical depth is low, this path length has a direct relationship with the cell-centered intensity. Thus, a new correction to the SC ray BC intensities, based on the path length discrepancy, was implemented. During grid intersection calculations, two additional lengths are stored for each cell's rays: path length from the plasma edge intersection to the ray's SC boundary (δBC), and path length from the plasma edge intersection to the "back" of the cell itself, i.e. including the full path through the entire cell (δF).

For plasma-edge cells, no correction is needed because the BCs are known. For all other cells, the BC intensity magnitude is scaled by the following ratio:

$$\frac{\delta\mathrm{BC(self)}}{\delta\mathrm{F(BC\ cell)}}$$

where "BC cell" refers to the cell just beyond the SC ray's terminating intersection point (whose intensity at the back, prior to the implementation of this correction, was used directly). The lengths used by the BC correction for the red ray in Figure 3 are labeled. The blue ray defines one of the three rays used for the BC for the red ray (since these rays are also tilted into the y-plane, the red ray's SC segment intersects the blue ray's start zone at point A since they are toroids). Note that, though these path lengths to the plasma edge are stored, radiation transfer is not calculated all the way along them as it would be with LC. Since a given cell and ray intensity can only be calculated once a BC is known, each BC intensity value is always pre-corrected. I.e., the path length used in the calculation of each BC intensity is scaled to the correct path length (from the plasma edge). This is why each succeeding cell only needs to scale by the BC cell's full path to the edge (as well as its own path from the plasma edge to the SC boundary). This scaling correction is done for each of the three rays contributing to the weighted average over angle.

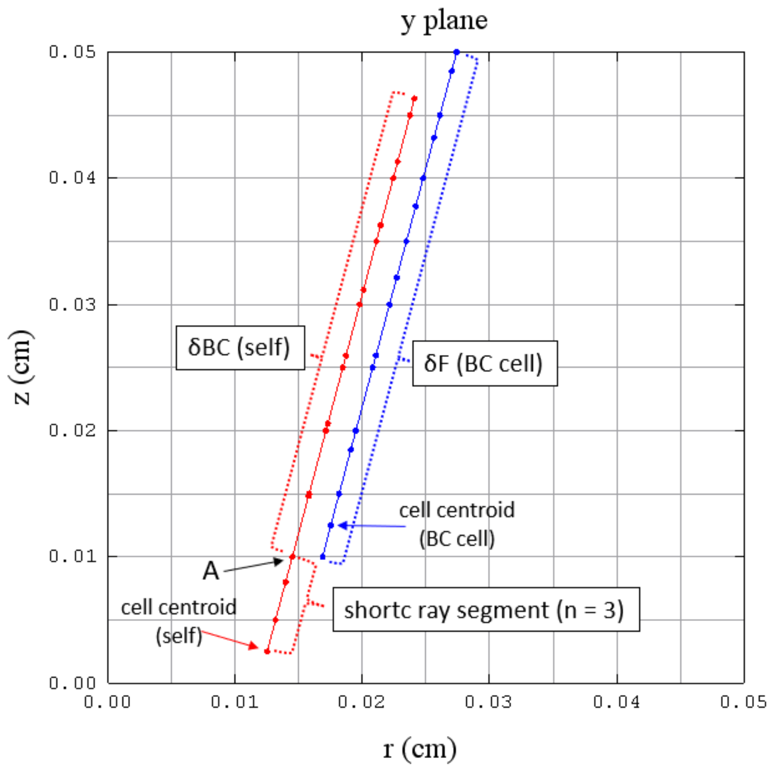

Figure 3. Lengths for the scaling factor when calculating intensity along the red ray, whose BC is defined in part by the blue ray.

Benchmarks

SC results are benchmarked against LC by plotting J/S for a single photon energy with constant opacity, where J is the solid angle average of intensity, and S is the source function. Firstly, the effect of the scaling technique is shown for a spherical plasma in 2DRZ geometry in Figure 4, where the constant opacity results in an optical depth (OD) from the center to the edge of (a) 0.1, (b) 1, (c) 3, (d) 10, and (e) 30. See that, in the optically thin case (a), the scaling correction results in nearly identical J/S for SC vs. LC, even with N = 3. When more absorption occurs over the photon's path, the scaling becomes less effective though at OD = 1 (b) it still gives better agreement for N = 3. For OD = 3 (c) and OD = 10 (d), accuracy is a little less with the scaling. When OD becomes high, the boundary conditions are no longer relevant, and the becomes irrelevant. In all cases, N = 9 is nearly identical to the LC case. However, for cases where optical depth is around this mid-range (3-10) for the important radiation, it may be preferrable to turn this scaling off. For low optical depth, the improvement is substantial.

More benchmarks are shown in Figures 5-8 for total OD = 1. Figure 5 is a cylindrical 2DRZ geometry, Figure 6 is a cylindrical 2DRZ geometry with finer gridding in the r dimension, Figure 7 is the same spherical 2DRZ geometry as in Figure 4, and Figure 8 is a 2DXY planar geometry. All of these cases show good agreement with the LC benchmark.

Full distributions of J/S per cell are shown in Figure 9 for the 2DRZ cylindrical geometry with coarser r-gridding, in Figure 10 for the 2DRZ cylindrical geometry with finer r-gridding, in Figure 11 for the 2DRZ spherical geometry, and in Figure 12 for the 2DXY geometry. Each figure shows the result for SC with N = 3 using the scaling technique (left), and for the LC benchmark (right). All cases show a very similar shape between SC and LC.

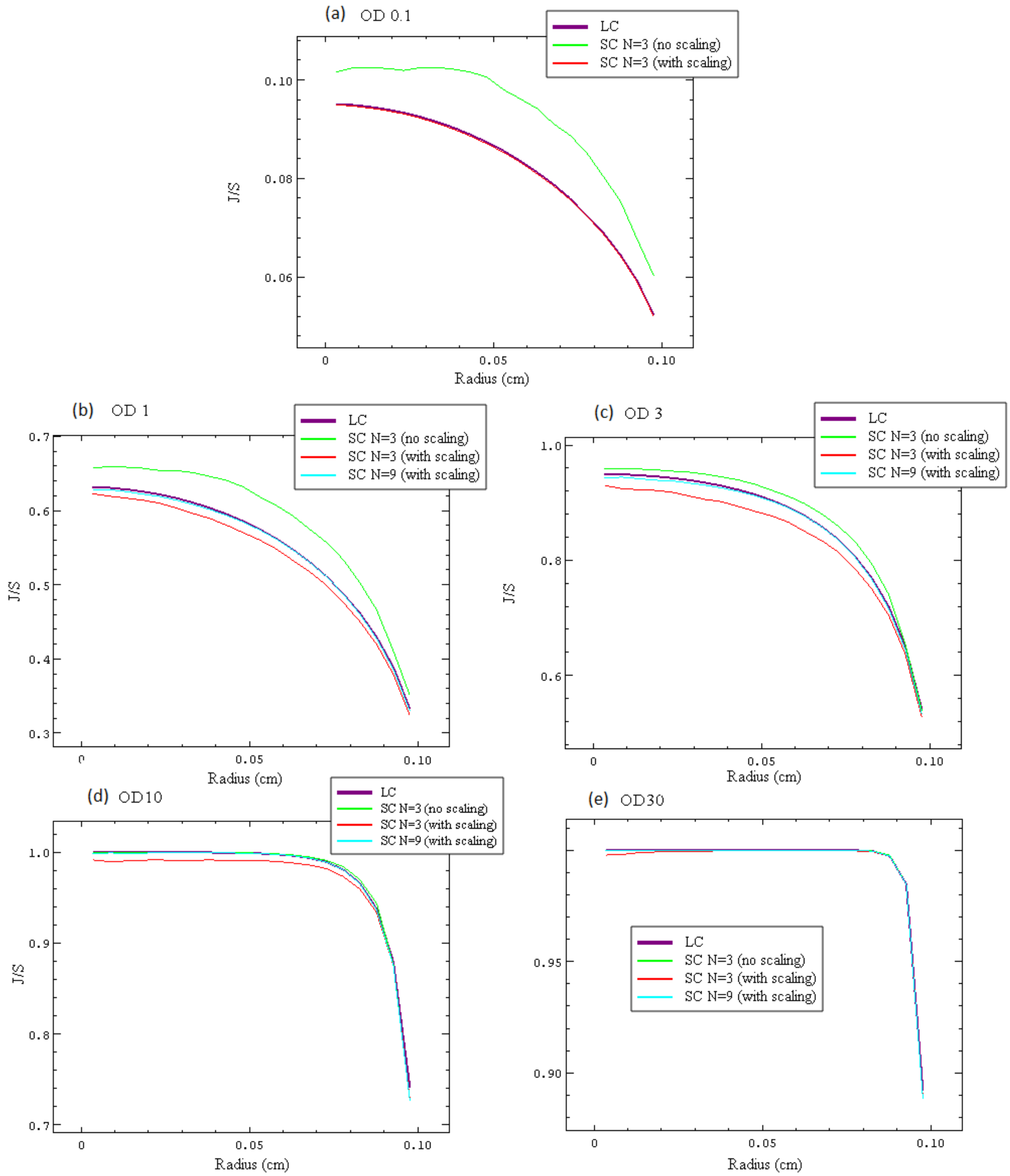

Figure 4. J/S benchmarks of SC, with and without the scaling, vs. the LC benchmark. Opacity is constant in each such that total OD is (a) 0.1, (b) 1, (c) 3, (d) 10, and (e) 30. Plasma is a sphere in 2DRZ geometry.

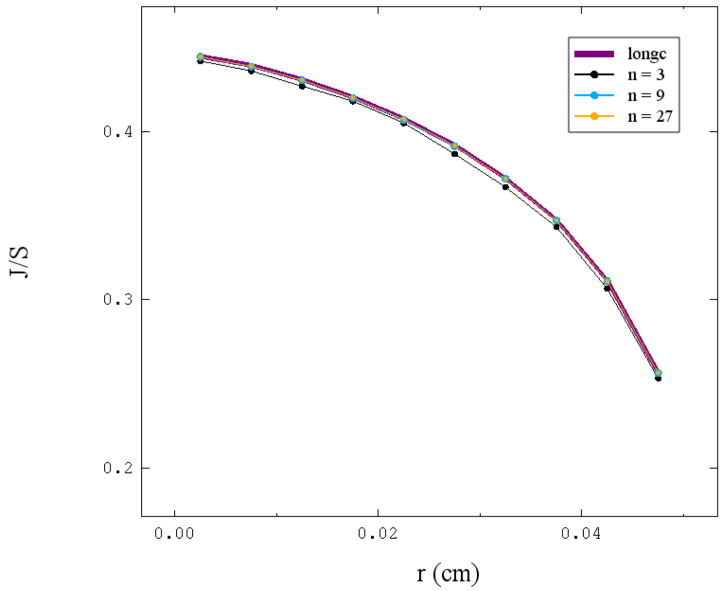

Figure 5. J/S lineouts for SC with n=3, n=9, and n=27, and LC, for a 2DRZ cylinder.

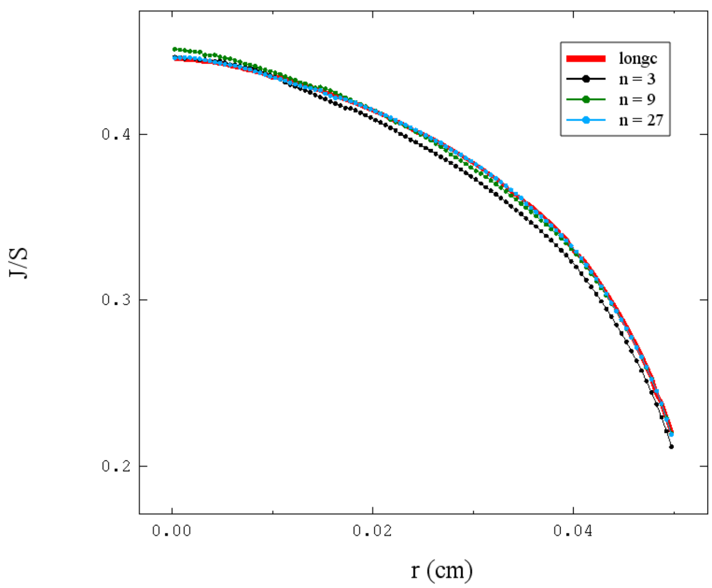

Figure 6. J/S lineouts for SC with n=3, n=9, and n=27, and LC, for a 2DRZ cylinder with fine r-gridding.

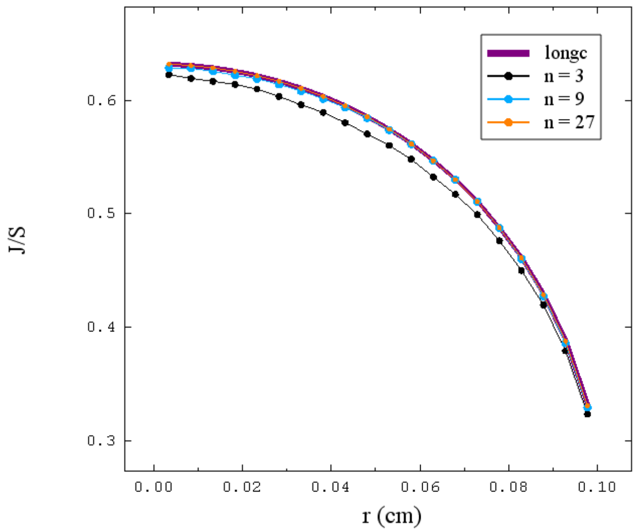

Figure 7. J/S lineouts for SC with n=3, n=9, and n=27, and LC, for a 2DRZ sphere.

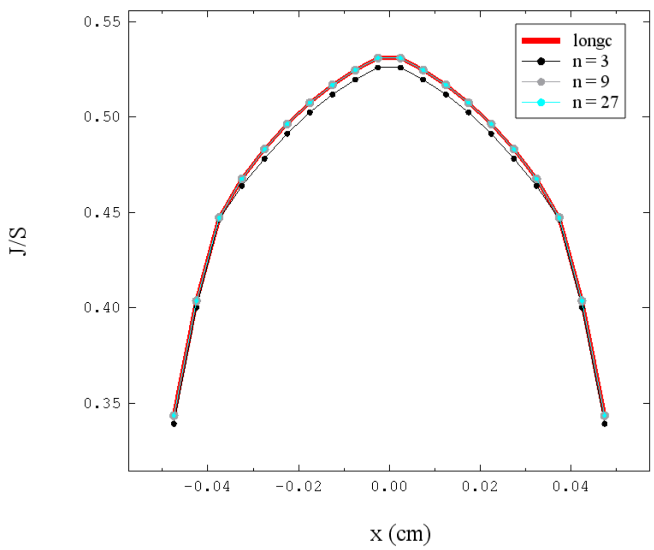

Figure 8. J/S lineouts for SC with n=3, n=9, and n=27, and LC, for a 2DXY planar geometry.

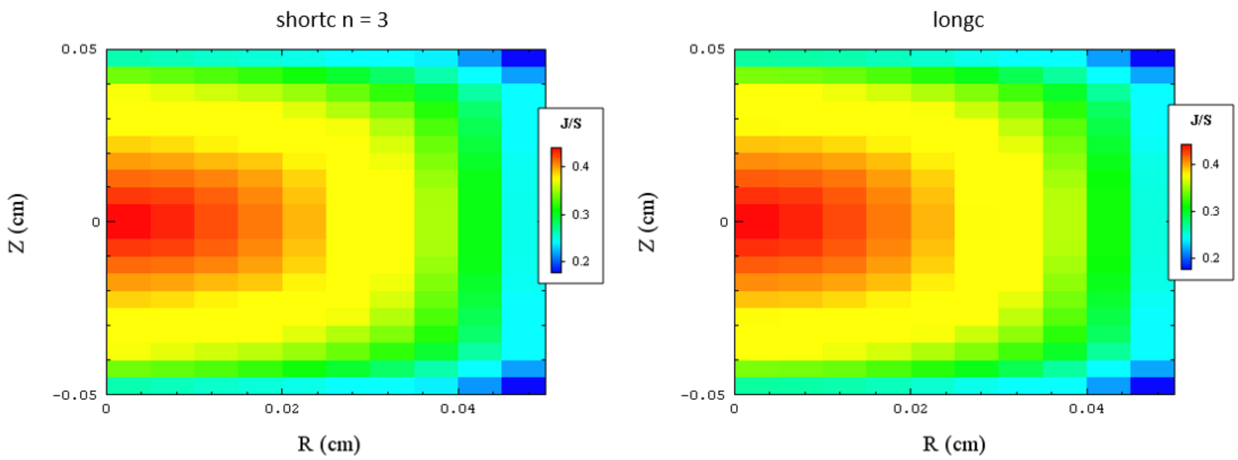

Figure 9. Full J/S distributions for SC with n=3 (left) and LC (right) for a 2DRZ cylinder with coarser r-gridding.

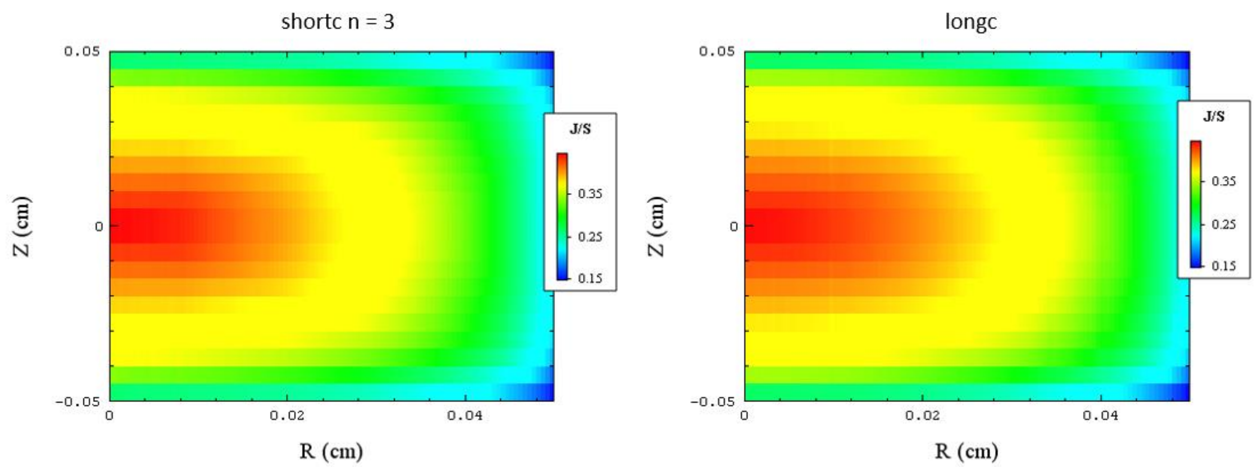

Figure 10. Full J/S distributions for SC with n=3 (left) and LC (right) for a 2DRZ cylinder with finer r-gridding.

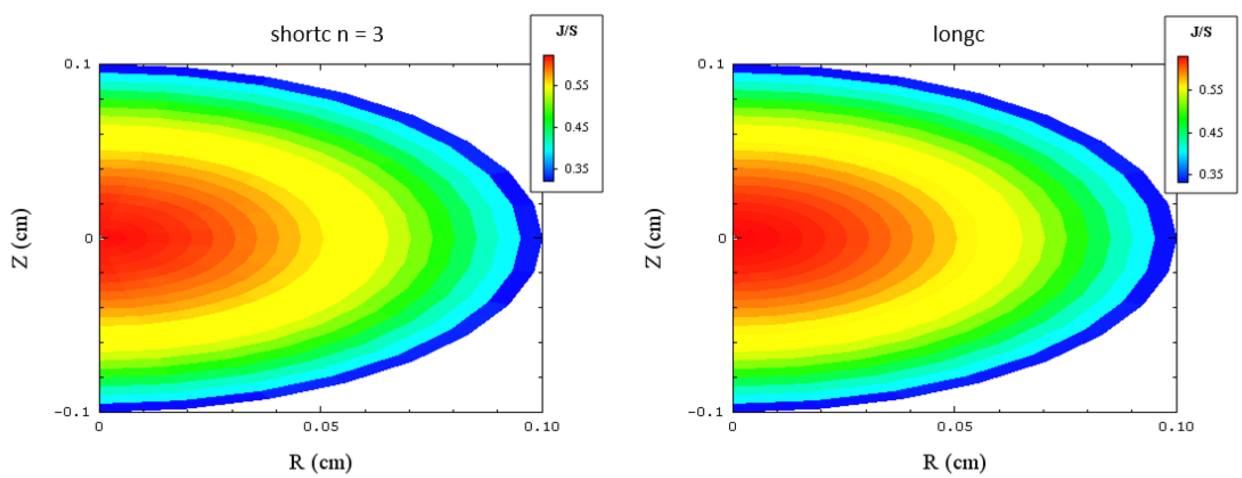

Figure 11. Full J/S distributions for SC with n=3 (left) and LC (right) for a 2DRZ sphere.

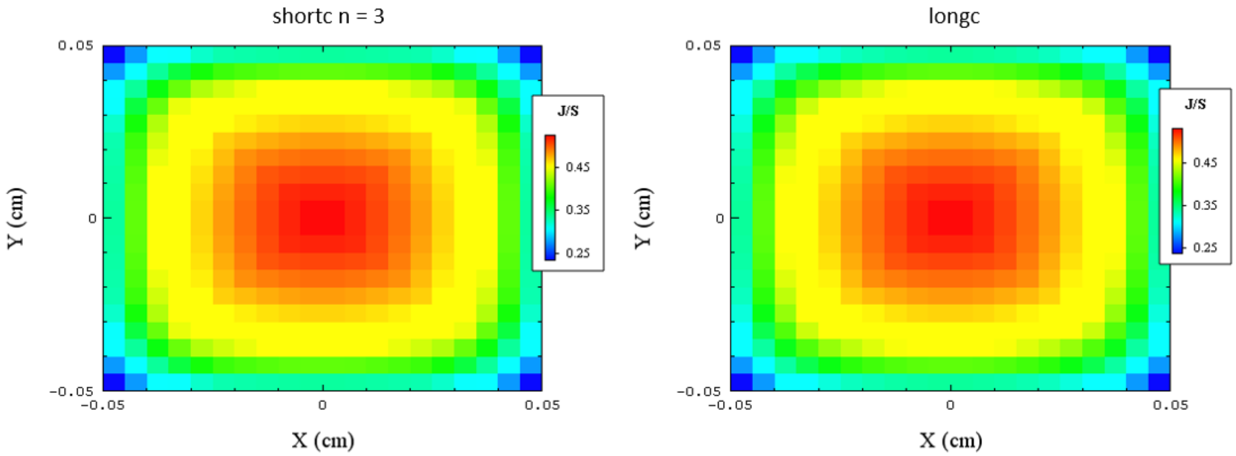

Figure 12. Full J/S distributions for SC with n=3 (left) and LC (right) for 2DXY.